

SOD/catalase conjugated with block ionomer - antioxidant delivery system

N.L. Klyachko¹, E.V. Batrakova², L.S. Shlyakhtenko², V. Kurova³, and A.V. Kabanov^{2,1}

¹ M.V.Lomonosov Moscow State University, Moscow, Russia

(klyachko@enzyme.chem.msu.ru)

² University of Nebraska Medical Center, Nebraska, Omaha, USA

³ N.M.Emanuel Institute of Biochemical Physics, Moscow, Russia



Introduction

One of the important components of metabolic and degenerative diseases of the nervous system involves inflammation that leads to excessive production of reactive oxygen species (ROS) playing crucial role in cell damage (neurodegeneration) and death (V.H. Perry, 1995). One of the neurodegenerative disorders in people over 65, Parkinson's disease (PD), involves brain inflammation, microglia activation and subsequent secretory neurotoxic activities, including ROS production. Superoxide dismutase (SOD) is capable to remove superoxide radical from reaction mixtures, by catalysing its dismutation to O₂ plus H₂O₂ (J.M. McCord, 1969). Catalase catalyses the decomposition of hydrogen peroxide to water and molecular oxygen being one of the fastest (highest turnover rates) biocatalysts serving to protect the cell from the toxic effects of hydrogen peroxide (M. Zamocky, 1999). In an *in vitro* model of PD, catalase was shown to rescue primary cerebellar granule cells from ROS toxic effects (R.A. Gonzalez-Polo, 2004). However, protein molecules should be protected from destabilization or/and disintegration by different enzymatic systems of organisms.

Different approaches are known to protect enzymes at nanoscale, for example, encapsulation them into nanoemulsions (N.L. Klyachko, 2003) or block-ionomer complexes (E.V.Batrakova, 2007). In the work presented, enzyme-polyelectrolyte complexes followed by chemical modification were prepared at the nanoscale. The resulted nanoparticles contain a core of protein-polyelectrolyte complex/conjugate surrounded by a shell of water soluble nonionic polymer such as polyethylene glycol (PEG) (fig. 1). Bi-enzyme antioxidant system comprising SOD and catalase working in a consecutive manner were encapsulated together in order to give more pronounced antioxidant effect. Comparison of physical-chemical and biochemical properties of the particles obtained has been done.

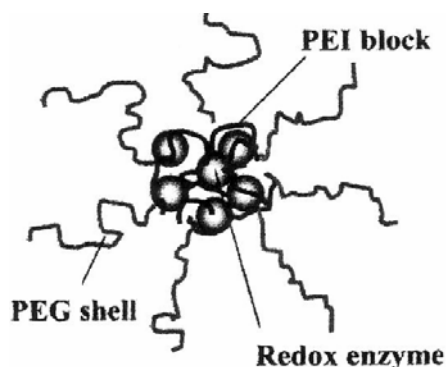


Figure 1: schematic representation of enzyme-containing polyethyleneimine - poly (ethylene glycol) (PEI-PEG) complex

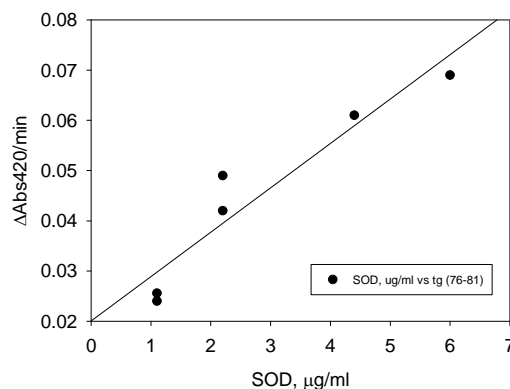


Figure 2: Dependence of the catalytic activity of SOD on the enzyme concentration

Materials and methods

Catalase from bovine liver, SOD from bovine erythrocytes, pyrogallol, TDPA, glutaraldehyde, bis-(sulfosuccinimidyl)suberate sodium salt (BS3), EDC, Tris, phosphate-buffered saline (PBS) were purchased from Sigma-Aldrich. PEI-PEG and polylysine-PEG (PL-PEG) block ionomers with molecular masses of 12 kDa and 7.6 kDa, respectively, were purchased from Alamanda Polymers (USA).

Block ionomer complexes. Given amount of catalase (2 mg/ml), SOD (2 mg/ml), PEI-PEG (1 mg/ml) and PL-PEG (2.6 mg/ml) were separately dissolved in PBS at RT. Enzyme solutions were mixed with polymer solutions under constant stirring. The +/- charge ratio (Z) was calculated by dividing the amount of amino groups of PEI-PEG or PL-PEG protonated at pH 7.4 by the total amount of Glu and Asp in protein molecules and was kept equal to ~1.

Chemical conjugation of enzyme/block ionomer complexes was carried out using glyceraldehyde (GA), N-ethyl-N'-(3-dimethylaminopropyl)-carbodiimide (EDC) or EDC/sulfo-NHS, and suberic acid bis(3-sulfo-N-hydroxysuccinimide ester) sodium salt (BS3). Enzyme/linker (NH₂ or COOH groups) molar ratios were varied from ¼ to 1/100, pH used were 7.4 (5.2 or 6.8 in some cases). Mixtures were incubated for 2h at RT or overnight at 4C. Schiff-base after GA modification was reduced using NaBH₄. All reaction mixtures were purified by gel-filtration procedure (Sephadex G-25) using NAP10 columns (Sigma).

SDS gel electrophoresis and western blot of enzyme/block ionomer conjugates. Enzyme/polymer conjugates were loaded in a 10% acrylamide gel with PBS, pH 7.4, under denaturing conditions. The protein bands were visualized with rabbit polyclonal anti-catalase or anti-SOD antibodies.

Light scattering measurements. Effective hydrodynamic diameters were measured by photon correlation spectroscopy (DLS) using 'ZetaPlus' Zeta Potential Analyzer (Brookhaven Instruments, Santa Barbara, CA) in a thermostatic cell at a scattering angle of 90°. All measurements were performed at 25°C.

Atomic Force Microscopy (AFM). Samples for AFM imaging were prepared by depositing 5ul of aqueous solutions of enzyme/polymer conjugates onto positively charged mica surface for 10 min, and then washing with water and drying under argon atmosphere. The AFM imaging was performed in air and liquid using a Multimode NanoScope IV system (Veeco, Santa Barbara, CA) operated in tapping mode. Images were processed and the widths of the particles were measured using Femtoscan software.

Enzyme activity measurements. Catalase and SOD activities in enzyme/polymer complexes and conjugates were studied using hydrogen peroxide decomposition (catalase) and pyrogallol (PG) oxidation followed by superoxide radical dismutation (SOD). Activities were measured by monitoring the change in absorbance at 240 nm (catalase) and 420 nm (SOD). As an example of catalase assay: to 1 ml 60 mM phosphate buffer, pH 7.4, 2 ul H₂O₂ and 1-6 ul catalase were added. As an example of SOD assay: to 1ml 60mM Tris, pH 8.2 + 1mM DPTA, 2ul PG (0.4M) was added into both cuvettes, 1-6 ul SOD was added then into reference cuvette. Linear dependence of SOD catalytic activity on the enzyme concentration (fig. 2) was observed. Similar linear dependence was found for catalase activity (not shown).

Results and discussion

As known, both enzymes represent oligomeric proteins dissociating in denaturing conditions (60 and 16 kDa for Cat and SOD, respectively, in figs 3 and 4). As found, complex formation (enzyme encapsulation by block ionomers) occurs even without linker at all (27) which is more pronounced in the case of SOD. GA (12, 13, 24) gives higher mol mass aggregates than other linkers, EDC (7, 8, 26, 32) and BS3 (18, 20, 31).

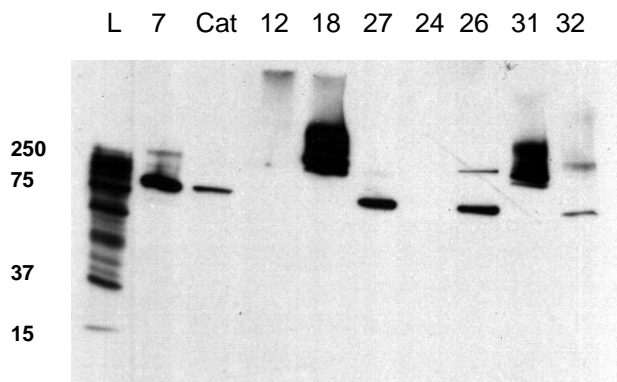


Figure 3: SDS-PAGE and catalase visualization by anti-catalase antibodies; 7 – Cat/PEI-PEG/EDC; 12 – Cat/PEI-PEG/GA; 18 – Cat/PEI-PEG/BS3; 27 – Cat-SOD/PEI-PEG/no linker; 24 – Cat-SOD/PEI-PEG/GA; 26 – Cat-SOD/PL-PEG/EDC; 31 – Cat-SOD/PL-PEG/BS3; 32 – Cat-SOD/PEI-PEG/EDC-S-NHS

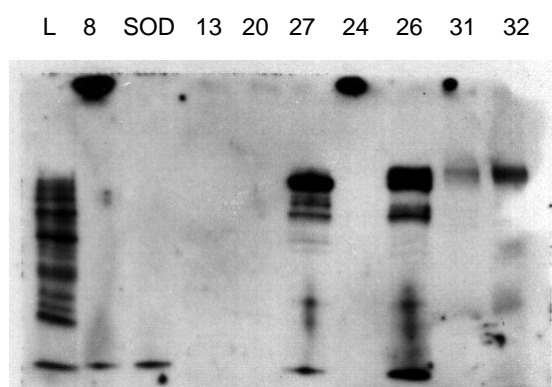


Figure 4: SDS-PAGE and SOD visualization by anti-SOD antibodies; 8 – SOD/PEI-PEG/EDC; 13– SOD/PEI-PEG/GA; 20 – SOD/PEI-PEG/BS3; 27 – Cat-SOD/PEI-PEG/no linker; 24 – Cat-SOD/PEI-PEG/GA; 26 – Cat-SOD/PL-PEG/EDC; 31 – Cat-SOD/PL-PEG/BS3; 32 – Cat-SOD/PEI-PEG/EDC-S-NHS

As seen, bands 12, 18, 31 represent non-dissociating particles where catalase/polymer complexes are chemically linked (26, 32 – are partially linked). Similar picture can be found with SOD (13, 20, 24, 26, 31, 32 bands represent linked protein aggregates and polymers).

To understand the effect of chemical modification on the enzyme function, catalytic properties of catalase and SOD were measured (fig. 5). As seen, both enzymes remain active after their complex formation with PEI-PEG. The catalase activity is more sensitive to pH (only 60% of residual activity retains at pH 6.8), SOD loses about 50% of its activity upon encapsulation in PL-PEG. Considering these values as initial ones, we can see almost no loss in the enzyme activity upon chemical modification (except GA effect on catalase (12, 24).

Sizes of the particles obtained were determined using DLS and AFM methods. As an example, fig. 6 shows the AFM image of catalase/PEI-PEG complex linked with BS3 (#18). As seen, 3 types of particles can be found: small (~17nm), medium (~24nm), and large (~40nm). In the table 1, sizes calculated from AFM images of several other samples are shown. As seen, 160 nm is the largest particle size obtained after modification. It is not surprising that the formation of smallest particles occurs upon SOD/catalase encapsulation in PL-PEG without chemical modification. To confirm that the whole complex (SOD/Cat/polymer) was linked, MALDI-TOF spectra were also analysed.

Our further experiments will examine the possibilities for nanoparticles transport to the areas of inflammation and other diseases and evaluate antioxidant protective effect in *in vivo* models.

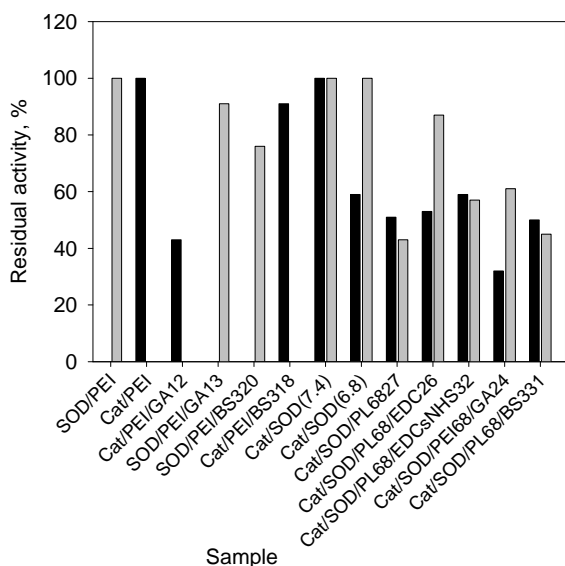


Figure 5: enzyme residual activity after complex with PEI-PEG or PL-PEG formation and chemical linking; catalase activity is shown in black, SOD activity is shown in grey

Conclusion

In the work done, enzyme polyelectrolyte complexes were prepared at the nanoscale by self-assembly of SOD and catalase with oppositely charged block ionomers. It became possible to fix antioxidant bi-enzyme system in such complexes by their chemical linking. In the resulting particles, antioxidant enzymes can be stabilized and delivered in the areas of inflammation.

Acknowledgement

N.L.K. is thankful for the financial support of her travel to Nebraska University Medical Center.

Bibliography

- V.H. Perry et al (2007) *Inflammation in the nervous system*. Curr. Opin. Neurobiol. 5, 636-641.
- J.J.M. McCord et al (1969) *Superoxide dismutase, an enzyme function for erythrocyte (hemocuprein)*. J. Biol. Chem. 244, 6049–6055.
- M. Zámocký (2004) *Phylogenetic relationships in class I of the superfamily of bacterial, fungal, and plant peroxidases*. Eur. J. Biochem. 271, 3297-3309.
- R.A.Gonzalez-Polo et al (2004) *Neuroprotection against MPP+ neurotoxicity in cerebellar granule cells by antioxidants*. Cell Biol. Int. 28, 373-380.
- N.L.Klyachko et al (2003). *Bioorganic synthesis in reverse micelles and related systems*. Curr. Opin. Colloid Int. Sci. 8, 179-186.
- E.V.Batrakova et al (2007) *A macrophage – nanozyme delivery system for Parkinson’s disease*. Bioconjugate Chem. 18, 1498-1506.

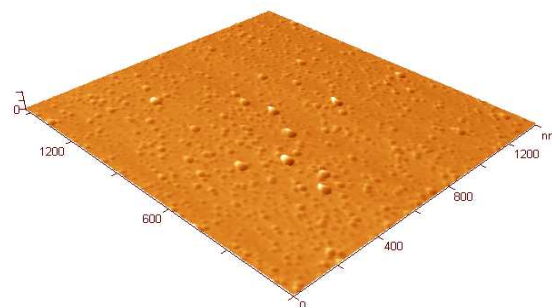


Figure 6: AFM image of catalase/PEI-PEG complex linked with BS3 (#18)

Sizes / N	12	18	26	27	31
Small	25	17	17	10	38
Medium	38	24	25	14	54
Large	60	40	38	17	160

Table 1: Sizes of particles found in AFM images of samples 12, 18, 26, 27, 31